

Synthesis, photophysics and electrochemistry of $[\text{Au}_2(\text{dppf})\text{R}_2]$ [$\text{dppf} = \text{Fe}(\eta\text{-C}_5\text{H}_4\text{PPh}_2)_2$; $\text{R} = \text{alkyl, aryl or alkynyl}$]. Crystal structure of $[\text{Au}_2(\text{dppf})(\text{C}_{16}\text{H}_9)_2]$ ($\text{C}_{16}\text{H}_9 = \text{pyren-1-yl}$)

Vivian Wing-Wah Yam,* Sam Wing-Kin Choi and Kung-Kai Cheung

Department of Chemistry, The University of Hong Kong, Pokfulam Road, Hong Kong

A series of organometallic complexes $[\text{Au}_2(\text{dppf})\text{R}_2]$ [$\text{dppf} = \text{Fe}(\eta\text{-C}_5\text{H}_4\text{PPh}_2)_2$; $\text{R} = \text{Me, Ph, 1-naphthyl, 9-anthryl, pyren-1-yl (C}_{16}\text{H}_9\text{), C}\equiv\text{CPh or C}\equiv\text{CBu}^1$] have been synthesized. Their photophysical and electrochemical properties have been studied. Both excimer and exciplex formation are evidenced in $[\text{Au}(\text{dppf})_2(\text{C}_{16}\text{H}_9)_2]$. The crystal structure of the latter has been determined.

Polynuclear d^{10} metal complexes have been shown to exhibit rich photo-physical and -chemical properties.^{1,2} However, most studies of this type have focused on simple Werner-type co-ordination complexes; in particular, those of gold(I) are relatively rare.^{2d,g,k,l} In addition, the well known antitumour, antirheumatoid arthritic and cytotoxic activities of gold(I) phosphine complexes,^{3a-c} together with the finding that ferrocenium salts could inhibit several solid tumours,^{3d} have prompted us to investigate the class of organometallic Au^{I} with 1,1'-bis(diphenylphosphino)ferrocene (dppf). Herein we report the synthesis, characterization and photophysical studies of a series of organometallic $[\text{Au}_2(\text{dppf})\text{R}_2]$ complexes ($\text{R} = \text{Me}$ **1**, **Ph** **2**, **1-naphthyl** **3**, **9-anthryl** **4**, **pyren-1-yl** **5**, $\text{C}\equiv\text{CPh}$ **6** or $\text{C}\equiv\text{CBu}^1$ **7**). The crystal structure of **5** will also be described.

Experimental

1,1'-Bis(diphenylphosphino)ferrocene (dppf), potassium tetrachloroaurate(III), 2,2'-thiodiethanol and methyllithium (1.4 mol dm^{-3} in diethyl ether) were obtained from Aldrich Chemical Company. The aryllithium reagents were prepared from *n*-butyllithium and the respective aryl bromide.⁴ The complex $[\text{Au}_2(\text{dppf})\text{Cl}_2]$ was prepared according to the literature procedure.^{5c} Tetra-*n*-butylammonium hexafluorophosphate (Aldrich, 98%) was purified by recrystallizing twice from absolute ethanol and dried under vacuum for 24 h before use. Diethyl ether was distilled over sodium-benzophenone and dichloromethane over calcium hydride before use. All other solvents and reagents were of analytical grade, used as received.

Synthesis of gold(I) complexes

All reactions were performed under strictly anhydrous and anaerobic conditions using standard Schlenk techniques under an atmosphere of nitrogen.

$[\text{Au}_2(\text{dppf})\text{Me}_2]$ **1.** To a suspension of $[\text{Au}_2(\text{dppf})\text{Cl}_2]$ (0.20 g, 0.20 mmol) in diethyl ether (20 cm^3) at -78°C was added a solution of 1.4 mol dm^{-3} methyllithium (84 cm^3 , 1.18 mmol). The mixture was allowed to warm slowly to room temperature during which the yellow suspension became clear and then turbid again shortly. After stirring for 18 h it was reduced in volume to ca. 5 cm^3 and CH_2Cl_2 (20 cm^3) was added. Filtration followed by removal of solvent and subsequent recrystallization from CH_2Cl_2 -light petroleum (b.p. $60\text{--}80^\circ\text{C}$) afforded complex **1** as orange crystals. Yield: 0.13 g, 65%. NMR (CD_2Cl_2): ^1H , δ 0.47 (s, 6 H, Me), 4.27 (s, 4 H, C_5H_4), 4.72 (s, 4 H, C_5H_4) and 7.36–7.56 (m, 20 H, PPh_2); ^{31}P , δ 41.8. Positive

FAB mass spectrum: $m/z = 963$, $[\text{M} - \text{Me}]^+$ (Found: C, 44.85; H, 3.55. Calc. for $\text{C}_{36}\text{H}_{34}\text{Au}_2\text{FeP}_2 \cdot 0.5\text{Et}_2\text{O}$: C, 44.7; H, 3.65%).

$[\text{Au}_2(\text{dppf})\text{Ph}_2]$ **2.** The procedure was similar to that above, except that 1.8 mol dm^{-3} phenyllithium (0.84 cm^3 , 1.18 mmol) was used instead of methyllithium. Recrystallization from CH_2Cl_2 -light petroleum afforded complex **2** as orange crystals. Yield: 0.15 g, 70%. NMR (CD_2Cl_2): ^1H , δ 4.38 (s, 4 H, C_5H_4), 4.83 (s, 4 H, C_5H_4), 7.36–7.63 (m, 10 H, Ph; 20 H, PPh_2); ^{31}P , δ 37.0. Positive FAB mass spectrum: $m/z = 1101$, M^+ ; 1025, $[\text{M} - \text{Ph}]^+$ (Found: C, 50.65; H, 3.35. Calc. for $\text{C}_{46}\text{H}_{38}\text{Au}_2\text{FeP}_2 \cdot 0.5\text{Et}_2\text{O}$: C, 50.4; H, 3.65%).

$[\text{Au}_2(\text{dppf})(\text{C}_{10}\text{H}_7)_2]$ **3.** The procedure was similar to that for $[\text{Au}_2(\text{dppf})\text{Me}_2]$, except that 1.0 mol dm^{-3} 1-naphthyllithium (1.0 cm^3 , 1.18 mmol) was used instead of methyllithium. Recrystallization from CH_2Cl_2 -light petroleum afforded complex **3** as orange needles. Yield: 0.17 g, 70%. ^1H NMR (CD_2Cl_2): δ 4.41 (s, 4 H, C_5H_4), 4.94 (s, 4 H, C_5H_4), 7.35–7.70 (m, 10 H, C_{10}H_7 ; 20 H, PPh_2), 7.80 (d, 2 H, C_{10}H_7) and 8.55 (d, 2 H, C_{10}H_7). Positive FAB mass spectrum: $m/z = 1077$, $[\text{M} - \text{C}_{10}\text{H}_7]^+$ (Found: C, 53.5; H, 3.55. Calc. for $\text{C}_{54}\text{H}_{42}\text{Au}_2\text{FeP}_2$: C, 53.9; H, 3.50%).

$[\text{Au}_2(\text{dppf})(\text{C}_{14}\text{H}_9)_2]$ **4.** The procedure was similar to that for $[\text{Au}_2(\text{dppf})\text{Me}_2]$, except that 1.0 mol dm^{-3} 9-anthryllithium (1.0 cm^3 , 1.18 mmol) was used instead of methyllithium. Recrystallization from CH_2Cl_2 -light petroleum afforded complex **4** as orange crystals. Yield: 0.18 g, 70%. ^1H NMR (CD_2Cl_2): δ 4.46 (s, 4 H, C_5H_4), 5.01 (s, 4 H, C_5H_4), 7.35–7.49 (m, 20 H, PPh_2) and 7.64–8.90 (m, 18 H, C_{14}H_9). Positive FAB mass spectrum: $m/z = 1303$, M^+ ; 1126, $[\text{M} - \text{C}_{14}\text{H}_9]^+$ (Found: C, 54.85; H, 3.50. Calc. for $\text{C}_{62}\text{H}_{46}\text{Au}_2\text{FeP}_2 \cdot \text{CH}_2\text{Cl}_2$: C, 54.5; H, 3.45%).

$[\text{Au}_2(\text{dppf})(\text{C}_{16}\text{H}_9)_2]$ **5.** The procedure was similar to that of $[\text{Au}_2(\text{dppf})\text{Me}_2]$, except that 1.0 mol dm^{-3} pyrenyllithium (1.0 cm^3 , 1.18 mmol) was used instead of methyllithium. Recrystallization from CH_2Cl_2 -light petroleum afforded complex **5** as orange crystals. Yield: 0.19 g, 70%. ^1H NMR (CD_2Cl_2): δ 4.48 (s, 4 H, C_5H_4), 4.98 (s, 4 H, C_5H_4) and 7.32–8.75 (m, 18 H, C_{16}H_9 ; 20 H, PPh_2). Positive FAB mass spectrum: $m/z = 1350$, M^+ ; 1150, $[\text{M} - \text{C}_{16}\text{H}_9]^+$ (Found: C, 58.75; H, 3.40. Calc. for $\text{C}_{66}\text{H}_{46}\text{Au}_2\text{FeP}_2$: C, 58.7; H, 3.40%).

$[\text{Au}_2(\text{dppf})(\text{C}\equiv\text{CPh})_2]$ **6.** To a suspension of $[\text{Au}_2(\text{dppf})\text{Cl}_2]$ (200 mg, 0.20 mmol) in ethanol (10 cm^3) was added an ethanolic

solution of a mixture of phenylacetylene (43 μl , 0.39 mmol) and sodium ethoxide (9 mg Na in 5 cm^3 EtOH). The resulting mixture was stirred for 5 h. The yellow solid was filtered off and washed successively with water, methanol and diethyl ether. Orange crystals of complex **6** were obtained by recrystallization from dichloromethane–hexane. Yield: 163 mg (75%). ^1H NMR (CD_2Cl_2): δ 4.33 (s, 4 H, C_5H_4), 4.77 (s, 4 H, C_5H_4) and 7.19–7.60 (m, 30 H, Ph). Positive FAB mass spectrum: $m/z = 1050$, M^+ . IR (Nujol): $\tilde{\nu}/\text{cm}^{-1}$ 2115vw ($\text{C}\equiv\text{C}$).

[Au₂(dppf)(C \equiv CBu)₂] **7**. The method was similar to that above, except that BuC \equiv CH (48 μl , 0.39 mmol) was used in place of PhC \equiv CH. Upon addition of the acetylide solution the yellow suspension changed at once into a clear yellow solution. After stirring for 5 h the solution was concentrated and addition of hexane to the yellow solution afforded [Au₂(dppf)(C \equiv CBu)₂] as yellow needles. Yield: 163 mg (75%). ^1H NMR (CD_2Cl_2): δ 1.33 (s, 18 H, Bu), 4.24 (s, 4 H, C_5H_4), 4.63 (s, 4 H, C_5H_4) and 7.34–7.52 (m, 20 H, PPh₂). Positive FAB mass spectrum: $m/z = 1109$, M^+ ; 1028, $[M - \text{C}\equiv\text{CBu}]^+$. IR (Nujol): $\tilde{\nu}/\text{cm}^{-1}$ 2115vw ($\text{C}\equiv\text{C}$).

Physical measurements and instrumentation

The UV/VIS spectra were obtained on a Hewlett-Packard 8452A diode-array spectrophotometer, IR spectra as Nujol mulls on a Bio-Rad FTS-7 spectrophotometer, and steady-state excitation and emission spectra on a Spex Fluorolog-2 111 fluorescence spectrofluorometer with or without Corning filters. Low-temperature (77 K) spectra were recorded using an optical Dewar sample holder. Proton and ^{31}P NMR spectra were recorded on a JEOL JNM-GSX270 multinuclear Fourier-transform spectrometer with chemical shifts reported relative to tetramethylsilane and 85% H_3PO_4 , respectively, and positive-ion FAB mass spectra on a Finnigan MAT95 spectrometer. Elemental analyses of the metal complexes were performed by Butterworth Laboratories Ltd.

Emission lifetime measurements were made using a conventional laser system. The excitation source was the 355 nm output (third harmonic) of a Quanta-Ray Q-switched GCR-150-10 pulsed Nd-YAG laser. Luminescence decay signals were recorded on a Tektronix TDS 620A digital oscilloscope and analysed using a program for exponential fits. All solutions for photophysical studies were prepared under vacuum in a round-bottom flask (10 cm^3) equipped with a sidearm 1 cm quartz fluorescence cuvette and sealed from the atmosphere by a Kontes quick-release Teflon stopper. Solutions were rigorously degassed with no fewer than four freeze–pump–thaw cycles. Steady-state photolysis experiments were performed using an Oriel 200 W mercury (xenon) lamp equipped with a water lens to remove IR radiation and a UV cut-off filter as the excitation source. The spectral changes during the course of the photolysis reaction were monitored by a Hewlett-Packard 8452A diode-array UV/VIS spectrophotometer. Solutions for preparative photolysis were prepared in glass tubes equipped with rubber septa and degassed by passage of high-purity nitrogen gas for 20 min. The degassed samples were irradiated using a Rayonet model RPR-100 photochemical chamber reactor with RPR-3500 Å lamps. In a typical experiment, a degassed dichloromethane solution of complex **6** (10^{-5} mol dm^{-3}) was irradiated for about 3 d at $\lambda = 350$ nm. The sample was then filtered and concentrated. Addition of diethyl ether to the concentrated dichloromethane solution precipitated the inorganic complex which was identified as [Au₂(dppf)Cl₂] and filtered off. The diethyl ether filtrate was concentrated and analysed by EI mass spectrometry (m/z 202, M^+) as PhC \equiv C–C \equiv CPh.

Cyclic voltammetric measurements were performed by using a Princeton Applied Research (PAR) universal programmer (model 175), potentiostat (model 173) and digital coulometer

(model 179). Cyclic voltammograms were recorded with a Kipp & Zonen BD90 X-Y recorder at scan rates of 200–50 mV s^{-1} . A conventional two-compartment electrolytic cell was used. The salt bridge of the reference electrode was separated from the working-electrode compartment by a Vycor glass. Electrochemical studies were performed in a non-aqueous medium (0.1 mol dm^{-3} NBu₄PF₆ in dichloromethane) with Ag–AgNO₃ (0.1 mol dm^{-3} in MeCN) as the reference electrode. The ferrocenium–ferrocene couple was used as the internal reference. The working electrode was a glassy carbon (Atomergic Chemetal V25) electrode with a piece of platinum gauze acting as the counter electrode. The working electrode was treated as reported previously.⁶

Crystallography

Diffraction-quality crystals of complex **5** were obtained by slow diffusion of diethyl ether vapour into a dichloromethane solution of the complex.

Crystal data. C₆₆H₄₆Au₂FeP₂, $M_r = 1350.82$, triclinic, space group $P\bar{1}$ (no. 2), $a = 11.255(4)$, $b = 13.484(4)$, $c = 9.406(2)$ Å, $\alpha = 104.92(2)^\circ$, $\beta = 91.99(3)^\circ$, $\gamma = 114.50(2)^\circ$, $U = 1238.8(7)$ Å³, $Z = 1$, $D_c = 1.811$ g cm^{-3} , $\mu(\text{Mo-K}\alpha) = 63.25$ cm^{-1} , $F(000) = 656$, $T = 298$ K.

An orange crystal of dimensions 0.15 \times 0.10 \times 0.25 mm was used for data collection at 25 °C on a Rigaku AFC7R diffractometer with graphite-monochromatized Mo-K α radiation ($\lambda = 0.71073$ Å) and ω – 2θ scans with ω –scan angle ($1.31 + 0.35 \tan \theta$)° at a scan speed of 16.0° min^{-1} [up to four scans for reflection with $I < 10\sigma(I)$]. Intensity data ($2\theta_{\text{max}} = 45^\circ$; h 0–12, k –13 to 13, l –10 to 10; three standard reflections measured every 300 showed no decay) were corrected for Lorentz-polarization effects, and empirical absorption corrections based on the ψ scan of four strong reflections (minimum and maximum transmission factors 0.716 and 1.000). Upon averaging the 3420 reflections, 3221 of which were uniquely measured ($R_{\text{int}} = 0.048$), 2792 with $I > 3\sigma(I)$ were considered observed and used in the structural analysis. The space group was determined from systematic absences and confirmed by the successful refinement of the structure which was solved by heavy-atom Patterson methods and expanded using Fourier techniques.⁷ The refinement was by full-matrix least squares using the software package TEXSAN⁸ on a Silicon Graphics Indy computer. Atom Fe(1) is at a centre of symmetry at the origin so that one asymmetric unit consists of half the other atoms of the molecule. All the 36 atoms were refined anisotropically and the hydrogen atoms placed at calculated positions with thermal parameters equal to 1.3 times that of the attached C atoms were not refined. Convergence for 322 variable parameters by least-squares refinement on F with $w = 4F_o^2/\sigma^2(F_o^2)$, where $\sigma^2(F_o^2) = [\sigma^2(I) + (0.016F_o^2)^2]$ for 2792 reflections with $I > 3\sigma(I)$ was reached at $R = 0.031$ and $R' = 0.038$ with a goodness of fit of 1.91; $(\Delta/\sigma)_{\text{max}} = 0.01$. The final Fourier-difference map was featureless, with maximum positive and negative peaks of 1.52 and 0.90 $\text{e} \text{ \AA}^{-3}$ respectively. Selected bond distances and angles are collected in Table 1.

Atomic coordinates, thermal parameters, and bond lengths and angles have been deposited at the Cambridge Crystallographic Data Centre (CCDC). See Instructions for Authors, *J. Chem. Soc., Dalton Trans.*, 1996, Issue 1. Any request to the CCDC for this material should quote the full literature citation and the reference number 186/148.

Results and Discussion

Reaction of [Au₂(dppf)Cl₂] with an excess of LiR in diethyl ether under strictly anaerobic conditions afforded [Au₂(dppf)R₂], isolated as air-stable orange crystals. All the newly synthesized complexes gave satisfactory elemental

analyses and have been characterized by ^1H NMR, IR and FAB mass spectrometry. Although crystal structures of $\text{Au}^{\text{I}}(\text{dppf})$ complexes have been reported previously,⁵ **5** represents the first of an organogold(I)-dppf complex. Fig. 1 shows a perspective drawing of the complex with atomic numbering. Basically, the structure is similar to that of $[\text{Au}_2(\text{dppf})\text{Cl}_2]$.^{5c} The Fe atom lies on a crystallographic centre, thus, the asymmetric unit is only half the formula unit. The two PPh_2 groups are oriented in an *anti* configuration which precluded any possible intramolecular $\text{Au}\cdots\text{Au}$ contacts [$\text{Au}(1)\cdots\text{Au}(1^*)$ 8.3315 Å]. Although the two cyclopentadienyl rings can rotate freely, a *syn* configuration is not observed in this and other reported non-chelating $\text{Au}(\text{dppf})$ complexes.⁵ The Au–P bond distance of 2.295(2) Å (Table 1) and the angle $\text{P}(1)\text{–Au}(1)\text{–C}(18)$ of $172.1(3)^\circ$, which is close to linearity and typical of sp hybridization at a gold(I) centre, are in the range found for other organogold(I) phosphine complexes.^{2g,h} The two P atoms were slightly displaced from

each cyclopentadienyl ring (away from the Fe atom) by 0.092 Å. In addition, the distance of the Fe atom from the planes of the cyclopentadienyl rings (1.656 Å) compares well with values reported for the ferrocene moieties.⁵ The Fe–C [2.033(8)–2.058(8) Å] and P–C distances [1.786(8)–1.833(8) Å] are normal. An interesting feature of the structure is that the dppf acts as a bridging instead of a chelating ligand, similar to the bonding mode of dmpm ($\text{Me}_2\text{PCH}_2\text{PMe}_2$) in $[\text{Au}_2(\text{dmpm})\text{R}_2]$.^{2d} From previous reports on the crystal structures of dppf-containing gold(I) complexes,^{5b,d,e} most have both P atoms bonded to the same Au atom to give three-co-ordinate gold(I). The chelating nature of the ligand has also been found in complexes of Mn^{I} ,^{9a} Pt^{II} ^{9b} and Ag^{I} .^{9c}

The electronic absorption spectral data of $[\text{Au}_2(\text{dppf})\text{R}_2]$ are summarized in Table 2. The spectra of complexes **2–5** are dominated by the $\pi\text{--}\pi^*$ absorption of the aromatic **R** groups. Fig. 2 shows the spectra of **4** and **5** in dichloromethane. Only absorptions characteristic of the dppf moiety were observed for **1** as no low-energy absorption due to methyl groups was possible. A similar absorption band at ca. 440 nm is observed for $[\text{Au}_2(\text{dppf})\text{Cl}_2]$. By comparing the spectra for $\text{R} = \text{Me}$ and aryl it was found that those for $[\text{Au}_2(\text{dppf})\text{R}_2]$ ($\text{R} = \text{aryl}$) were simply the sum of the absorptions of the dppf moiety and of the aromatic groups. On the other hand, both complexes **6** and **7** show intense vibronically structured bands at 270–295 nm with progression spacings of ca. 1825 cm^{-1} , typical of intraligand $\pi\text{--}\pi^*$ ($\text{C}\equiv\text{C}$) transitions.

Excitation of $[\text{Au}_2(\text{dppf})\text{R}_2]$ at $\lambda > 330\text{ nm}$ gave weak emissions in dichloromethane solutions, whereas the complexes are non-emissive in the solid state at both room temperature and 77 K. The emission data, together with those of free dppf, are collected in Table 2. Fig. 3 shows the emission spectra of **4** and **5** in dichloromethane which are characterized by a vibronically structured emission together with a broader structureless band overlapping it. The vibrational progressions with spacings of ca. 1200 cm^{-1} , typical of the skeletal vibrational

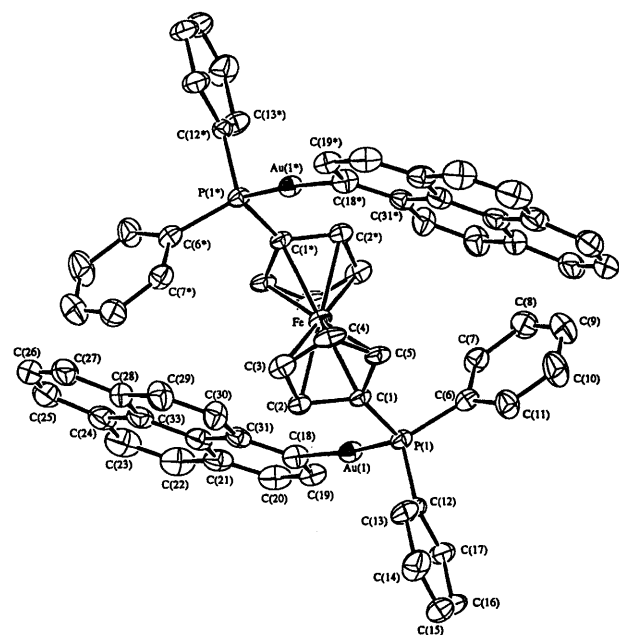


Fig. 1 Perspective view of $[\text{Au}_2(\text{dppf})(\text{C}_{16}\text{H}_9)_2]$ **5** with the atomic numbering scheme. Thermal ellipsoids are at the 30% probability level. Starred atoms have coordinates at $-x$, $-y$, $-z$

Table 1 Selected bond distances (Å) and angles ($^\circ$) for complex **5** with estimated standard deviations in parentheses

Au(1)–P(1)	2.295(2)	P(1)–C(6)	1.804(9)
Au(1)–C(18)	2.061(8)	P(1)–C(12)	1.833(8)
P(1)–C(1)	1.786(8)		
P(1)–Au(1)–C(18)	172.1(3)	Au(1)–P(1)–C(12)	116.5(3)
Au(1)–P(1)–C(1)	108.3(3)	Au(1)–C(18)–C(19)	122.5(7)
Au(1)–P(1)–C(6)	119.2(3)	Au(1)–C(18)–C(31)	119.7(6)

Table 2 Cyclic voltammetric, electronic absorption and emission data of $[\text{Au}_2(\text{dppf})\text{R}_2]$ in dichloromethane at 298 K

Complex	$\lambda_{\text{abs}}/\text{nm}$ ($\epsilon/\text{dm}^3\text{ mol}^{-1}\text{ cm}^{-1}$)	$\lambda_{\text{em}}/\text{nm}$	$E_{\text{pa}}^*/\text{V vs. SCE}$
1	266 (sh) (15 295), 438 (290)	408	+0.76 (+1.01)
2	274 (sh) (17 475), 306 (sh) (3875), 438 (315)	419	+0.74 (+1.03), +2.05
3	284 (24 635), 298 (27 580), 308 (20 625), 322 (5055), 442 (290)	367	+0.78 (+1.05), +1.66, +1.73, +1.88
4	256 (sh) (138 125), 263 (193 715), 378 (23 755), 436 (sh) (340)	408	+0.74 (+1.05), +1.27, +1.39, +1.54, +1.70
5	274 (56 345), 282 (69 565), 360 (79 740), 442 (sh) (235)	421	+0.66 (+1.08), +1.97
6	258 (37 215), 270 (51 920), 284 (52 140), 292 (29 770), 310 (3195), 442 (190)	410	+0.95 (+1.11)
7	254 (sh) (47 545), 270 (41 195), 282 (35 735), 292 (23 575), 442 (210)	410	+0.93 (+1.11)
dppf		403	(+0.97)

* In dichloromethane (0.1 mol dm^{-3} NBu_4PF_6). Working electrode, glassy carbon; scan rate, 100 mV s^{-1} ; potentials in parentheses refer to quasi-reversible couples.

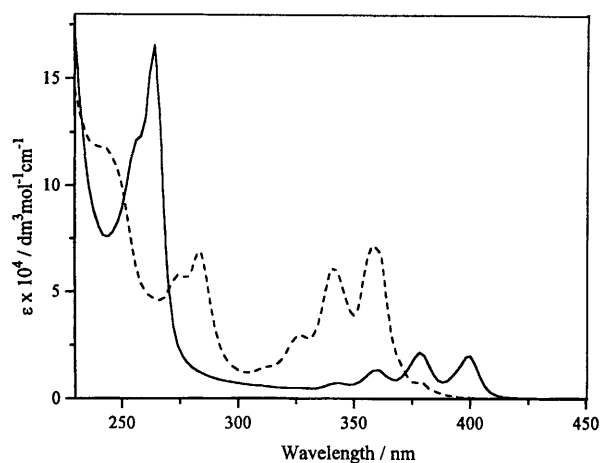


Fig. 2 Electronic absorption spectra of complexes **4** (—) and **5** (---) in CH_2Cl_2 at 298 K

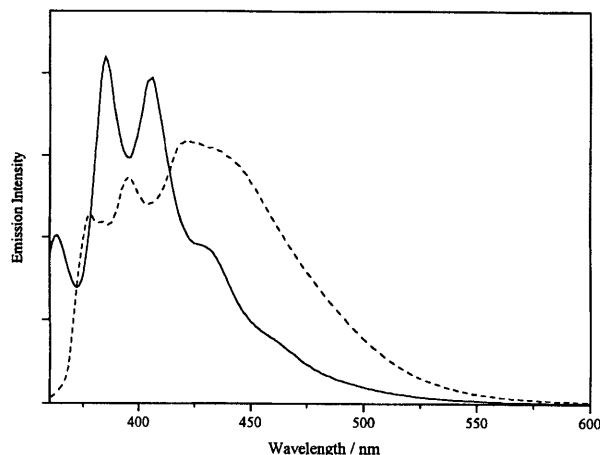


Fig. 3 Emission spectra of complexes **4** (—) and **5** (---) in CH_2Cl_2 at 298 K

modes of the aromatic rings, are assigned as intraligand $^3(\pi-\pi^*)$ emission of the anthryl and pyrenyl groups. The origin of the broad band is likely to be a dppf-centred $\sigma \rightarrow \pi^*$ transition (σ denotes the P–Au bond and π^* refers to the π^* orbital of the dppf ligand), which is relatively unperturbed upon incorporation of the gold and R moieties. Comparing the emission of $[\text{Au}_2(\text{dppf})\text{R}_2]$ (R = aryl) with that of the corresponding free aromatic hydrocarbons, the relative luminescence quantum yields of the former were much smaller than those of the latter. The excited state of the polyaromatic chromophore could be intramolecularly quenched by ferrocenyl groups *via* reductive electron transfer or energy-transfer quenching, resulting in a reduced luminescence quantum yield.

In order to investigate the possibility of excimer formation for complex **5**, concentration-dependence studies on the emission were performed. At concentrations of about $10^{-5} \text{ mol dm}^{-3}$ the emission is composed of pyrene monomer emission (*ca.* 400 nm). As the concentration increases two effects are observed: (i) the monomer emission diminishes and (ii) a new emission, due to the pyrene excimer, appears to the red of the monomer emission (*ca.* 500 nm) with the intensity increasing with increasing concentration. When the concentration reaches $3.53 \times 10^{-4} \text{ mol dm}^{-3}$ there is hardly any monomeric emission. Similar findings have been reported for related excimeric systems.¹⁰ The excimer formation is believed to be intermolecular in origin, though there are two pyrenyl groups in a single molecule of **5**, which even if they are in the *syn* configuration, would be too far apart to show excimeric interaction. When an excess of *N,N*-dimethylaniline is added to a dichloromethane solution of **5** the luminescence of the pyrene moiety at *ca.* 390 and 426 nm is quenched, accompanied by the concomitant appearance of a broad structureless band at *ca.* 490 nm (Fig. 4). The newly formed band is about 5200 cm^{-1} to the red of the luminescence of the pyrene moiety of **5** and its emission intensity increases as the aniline concentration increases, consistent with an assignment of exciplex formation.

Fig. 5 shows the spectral changes of a degassed dichloromethane solution of complex **6** upon steady-state irradiation with $\lambda > 330 \text{ nm}$. The traces show clean isosbestic points at 252 and 306 nm. The absorbances of the structured bands at 270 and 284 nm diminish along with a growth in absorption at *ca.* 246 nm. The organic product isolated after photolysis has been identified as the C–C coupling product $\text{Ph}-\text{C}\equiv\text{C}-\text{C}\equiv\text{CPh}$, and the inorganic product as $[\text{Au}_2(\text{dppf})\text{Cl}_2]$. It is proposed that upon irradiation of light the Au–C bond in **6** is activated and homolytic cleavage occurs by which the $\cdot\text{C}\equiv\text{CPh}$ radicals couple together to form the C–C coupling product. Both thermal and photoinduced C–C coupling reactions in gold(i) complexes have been reported.^{2j,11}

The incorporation of redox-active ferrocenyl groups in $[\text{Au}_2(\text{dppf})\text{R}_2]$ should also lead to interesting electrochemistry for this series of complexes. The electrochemical data are

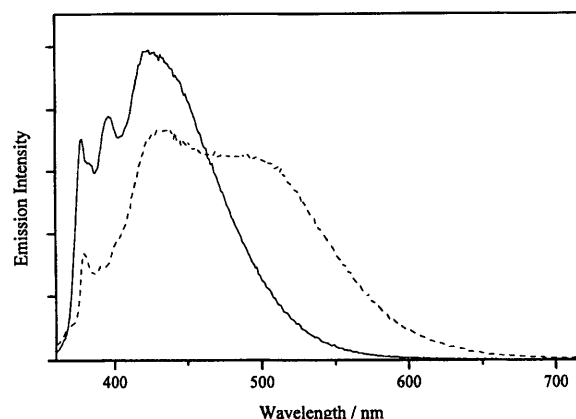


Fig. 4 Emission spectra of complex **5** ($1.13 \times 10^{-5} \text{ mol dm}^{-3}$) in the presence of 0 (—) and 0.12 mol dm^{-3} (---) *N,N*-dimethylaniline in CH_2Cl_2 at 298 K

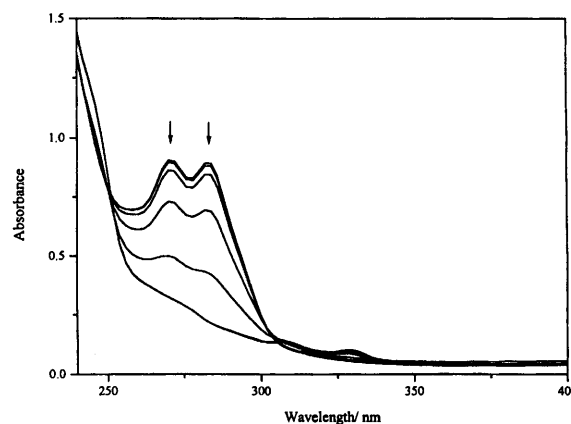


Fig. 5 Electronic absorption spectra of complex **6** in degassed CH_2Cl_2 solution upon irradiation at $\lambda > 350 \text{ nm}$

collected in Table 2. All the complexes studied showed quasi-reversible oxidation couples in the range 0.97–1.11 V *vs.* saturated calomel electrode (SCE). It is likely that this oxidation couple is dppf based, as evidenced from its occurrence at similar potentials to those observed for other dppf-substituted complexes.^{5b} Besides, irreversible anodic waves appeared at 0.66–0.95 V *vs.* SCE for $[\text{Au}_2(\text{dppf})\text{R}_2]$. With reference to our studies on the electrochemistry of other gold(i) complexes, the oxidation wave could be tentatively assigned as arising from a $\text{Au}^{\text{I}} \rightarrow \text{Au}^{\text{II}}$ oxidation. The absence of such irreversible oxidation waves in $[\text{Au}_2(\text{dppf})\text{Cl}_2]$ and other related Au–dppf complexes^{5b} probably stems from the different σ -donating abilities of the ligands. It is likely that such $\text{Au}^{\text{I}} \rightarrow \text{Au}^{\text{II}}$ oxidation processes are thermodynamically less favourable in the chloro counterparts and would only occur at very positive potentials, beyond the limit of the solvent windows. The anodic shift of the $E_{\text{f}}(\text{Au}^{\text{II}}-\text{Au}^{\text{I}})$ values of **6** and **7** relative to **1–5** is also in accord with the more electronegative sp-hybridized acetylenic carbon attached to the gold(i) centre in the former, which renders the centre less electron rich and more difficult to oxidize. With the exception of **1**, **6** and **7**, additional irreversible anodic waves are observable in the region of +1.27 to +2.05 V *vs.* SCE for $[\text{Au}_2(\text{dppf})\text{R}_2]$. It is likely that such oxidation processes involve the highly conjugated aryl rings.

Acknowledgements

V. W.-W. Y. acknowledges financial support from the Research Grants Council, the Croucher Foundation and The University of Hong Kong. S. W.-K. C. acknowledges the receipt of a Postgraduate Studentship, administered by The University of Hong Kong.

References

- 1 P. D. Harvey, F. Adar and H. B. Gray, *J. Am. Chem. Soc.*, 1988, **111**, 1312; P. D. Harvey and H. B. Gray, *J. Am. Chem. Soc.*, 1988, **110**, 2145; C. King, J. C. Wang, M. N. I. Khan and J. P. Fackler, jun., *Inorg. Chem.*, 1989, **28**, 2145; H. R. C. Jaw, M. M. Savas, R. D. Rogers and W. R. Mason, *Inorg. Chem.*, 1989, **28**, 1028; M. N. I. Khan, C. King, D. D. Heinrich, J. P. Fackler jun. and L. C. Porter, *Inorg. Chem.*, 1989, **28**, 2150; H. R. C. Jaw, M. M. Savas and W. R. Mason, *Inorg. Chem.*, 1989, **28**, 4366; T. M. McCleskey and H. B. Gray, *Inorg. Chem.*, 1992, **31**, 1733; D. M. Knotter, G. Blasse, J. P. M. van Vliet and G. van Koten, *Inorg. Chem.*, 1992, **31**, 2196; P. C. Ford and A. Vogler, *Acc. Chem. Res.*, 1993, **26**, 220; I. J. B. Lin, J. M. Hwang, D. F. Feng, M. C. Cheng and Y. Wang, *Inorg. Chem.*, 1994, **33**, 3467.
- 2 (a) C. M. Che, H. L. Kwong, V. W. W. Yam and K. C. Cho, *J. Chem. Soc., Chem. Commun.*, 1989, 885; (b) C. M. Che, H. L. Kwong, C. K. Poon and V. W. W. Yam, *J. Chem. Soc., Dalton Trans.*, 1990, 3215; (c) V. W. W. Yam, T. F. Lai and C. M. Che, *J. Chem. Soc., Dalton Trans.*, 1990, 3747; (d) V. W. W. Yam and S. W. K. Choi, *J. Chem. Soc., Dalton Trans.*, 1993, 2057; (e) V. W. W. Yam, W. K. Lee and T. F. Lai, *Organometallics*, 1993, **12**, 2383; (f) V. W. W. Yam, W. K. Lee and T. F. Lai, *J. Chem. Soc., Chem. Commun.*, 1993, 1571; (g) T. E. Müller, S. W. K. Choi, D. M. P. Mingos, D. Murphy, D. J. Williams and V. W. W. Yam, *J. Organomet. Chem.*, 1994, **484**, 209; (h) V. W. W. Yam, S. W. K. Choi and K. K. Cheung, *Organometallics*, 1996, **15**, 1734; (i) V. W. W. Yam and W. K. Lee, *J. Chem. Soc., Dalton Trans.*, 1993, 2097; (j) D. Li, C. M. Che, H. L. Kwong and V. W. W. Yam, *J. Chem. Soc., Dalton Trans.*, 1992, 3325; (k) D. Li, H. Xiao, C. M. Che, W. C. Lo and S. M. Peng, *J. Chem. Soc., Dalton Trans.*, 1993, 2929; (l) H. Xiao, K. K. Cheung, C. X. Guo and C. M. Che, *J. Chem. Soc., Dalton Trans.*, 1994, 1867.
- 3 (a) C. K. Mirabelli, D. T. Hill, L. F. Faucette, F. L. McCabe, G. R. Girard, D. B. Bryan, B. M. Sutton, J. O. Bartus, S. T. Crooke and R. K. Johnson, *J. Med. Chem.*, 1987, **30**, 2181; (b) S. J. Berners-Price, P. S. Jarret and P. J. Sadler, *Inorg. Chem.*, 1987, **26**, 3074; (c) O. M. N. Dhubhghaill, P. J. Sadler and R. Kuroda, *J. Chem. Soc., Dalton Trans.*, 1990, 2913; (d) P. Kopf-Maier and H. Kopf, *Chem. Rev.*, 1987, **87**, 1137.
- 4 J. A. Ladd and J. Parker, *J. Chem. Soc., Dalton Trans.*, 1972, 930.
- 5 (a) M. Viotte, B. Gautheron, M. M. Kubicki, Y. Mugnier and R. V. Parish, *Inorg. Chem.*, 1995, **34**, 3465; (b) C. Gimeno, A. Laguna, C. Sarroca and P. G. Jones, *Inorg. Chem.*, 1993, **32**, 5926; (c) D. T. Hill, G. R. Girard, F. L. McCabe, R. K. Johnson, P. D. Stupik, J. H. Zhang, W. M. Reiff and D. S. Eggleston, *Inorg. Chem.*, 1989, **28**, 3529; (d) L. T. Phang, T. S. A. Hor, Z. Y. Zhou and T. C. W. Mak, *J. Organomet. Chem.*, 1994, **469**, 253; (e) A. Houlton, D. M. P. Mingos, D. M. Murphy, D. J. Williams, L. T. Phang and T. S. A. Hor, *J. Chem. Soc., Dalton Trans.*, 1993, 3629.
- 6 C. M. Che, K. Y. Wong and F. C. Anson, *J. Electroanal. Chem. Interfacial Electrochem.*, 1987, **226**, 211.
- 7 PATTY and DIRDIF 92, P. T. Beurskens, G. Admiraal, G. Beurskens, W. P. Bosman, S. Garcia-Granda, R. O. Gould, J. M. M. Smits and C. Smykalla, The DIRDIF program system, Technical Report of the Crystallography Laboratory, University of Nijmegen, 1992.
- 8 TEXSAN, Crystal Structure Analysis Package, Molecular Structure Corporation, Houston, TX, 1985 and 1992.
- 9 (a) S. Onaka, M. Haga, S. Takagi, M. Otsuka and K. Mizuno, *Bull. Chem. Soc. Jpn.*, 1994, **67**, 2440; (b) W. R. Cullen, T. J. Kim, F. W. B. Einstein and T. Jones, *Organometallics*, 1983, **2**, 714; 1985, **4**, 346; (c) M. C. Gimeno, P. G. Jones, A. Laguna and C. Sarroca, *J. Chem. Soc., Dalton Trans.*, 1995, 1473.
- 10 T. Forster, *Angew. Chem., Int. Ed. Engl.*, 1969, **8**, 333; B. J. Birks, *Photophysics of Aromatic Molecules*, Wiley, New York, 1970.
- 11 A. Tamaki and J. K. Kochi, *J. Organomet. Chem.*, 1973, **61**, 441.

Received 1st May 1996; Paper 6/03086F